

A RADIO COUNTERPART FOR THE UNIDENTIFIED TEV SOURCE HESS J1813-178: THE RADIO-GAMMA-RAY CONNECTION

DAVID J. HELFAND

Columbia Astrophysics Laboratory, Columbia University, 550 West 120th Street, New York, NY 10027, USA

ROBERT H. BECKER

Physics Department, University of California, 1 Shields Avenue, Davis, CA 95616;
and Institute of Geophysics and Planetary Physics, Lawrence Livermore National Laboratory, Livermore, CA 94550

AND

RICHARD L. WHITE

Space Telescope Science Institute, 3700 San Martin Drive, Baltimore, MD 21218

Submitted to Astrophysical Journal Letters

ABSTRACT

We discovered independently the shell-type supernova remnant G12.82–0.02, recently reported by Brogan et al. (2005), which is coincident with the unidentified TeV gamma-ray source revealed in the HESS survey of the Galactic plane. Estimating the ambient starlight at the location of this source from the integrated Ly α luminosity of the nearby H II region W33, we conclude that inverse Compton emission is a viable explanation for the observed TeV emission. Examining remnants in the survey of Aharonian et al. (2005a) including those detected above 200 GeV *and* those not detected, we find a strikingly large range of more than three orders of magnitude in the radio to TeV flux ratios. We briefly explore the possible explanations of this range and the implications for the TeV emission mechanism.

Subject headings: supernova remnants — gamma rays: observations — radio continuum: ISM — H II regions — ISM: individual (G12.82–0.02) — gamma rays: theory

1. INTRODUCTION

The sites of cosmic ray acceleration in the Galaxy are widely believed to be supernova remnants (SNRs), although the evidence for this belief has been largely indirect. Over the last twenty years, nonthermal X-ray emission has been detected in several remnants, allowing us to infer that electrons with energies up to at least 100 TeV are present (e.g., Cas A – Allen et al. 1997; SN1006 – Becker et al. 1980; Koyama et al. 1995; G347.3–0.5 – Slane et al. 1999). Recently, the commissioning of the High Energy Stereoscopic System (HESS) for the detection of TeV gamma rays (Benbow et al. 2005) has opened a new window on high energy processes in the Galaxy, providing a tool to locate directly hadronic CR acceleration sites. A HESS survey of the innermost 60 degrees of Galactic longitude has recently been published (Aharonian et al. 2005a), and the results suggest we have much to learn about the details of CR acceleration in SNRs.

Of the ten discrete TeV-emitting sources found within the survey area ($-30^\circ < l < 30^\circ$, $|b| < 3^\circ$) only half have plausible identifications in existing source catalogs: the Galactic Center itself Sgr A* (Aharonian et al. 2004a), the X-ray synchrotron-dominated shell-type SNR RX J1713.7-3946 (Muraishi et al. 2000; Aharonian 2004b), and three new sources coincident with cataloged SNRs – HESS J1640-465 with G338.3–0.0, HESS J1804-216 with G8.7–0.1, and HESS J1834-087 with G23.3–0.3 – although, given the inexact spatial coincidences and a probability of $> 50\%$ for at least one chance HESS-SNR coincidence, not all of these identifications are secure.¹ Even

more interesting is the fact that there are an additional 88 catalogued remnants (from Green 2004) in the survey area, none of which are seen. While the detected remnants G8.7–0.1 and G23.3–0.3 rank third and fifth, respectively, in radio flux density at 1 GHz among known SNRs in the survey area, G338.3–0.0 ranks only 42nd, and G12.82–0.02 (discussed below) would rank 86th. Even given the possibility of a false identification, it is clear that a bright radio flux density is neither necessary nor sufficient to ensure detected TeV gamma rays.

2. A FAINT NEW SNR

We are in the process of constructing a Multi-Array Galactic Plane Imaging Survey (MAGPIS) with the Very Large Array² operating at a wavelength of 20 cm (D. J. Helfand et al., 2005, in preparation³). The images, constructed from B-, C-, and D-configuration observations plus single-dish data from the Effelsberg Galactic plane survey (Reich, Reich & Fuerst 1990) have a resolution of $\sim 5''$, a sensitivity over most of the area of $\sim 1-2$ mJy, and a dynamic range of $\sim 1000:1$. The longitude range covered to date ($32^\circ > l > 5^\circ$) includes five of the ten sources in the HESS Galactic plane survey.

Figure 1 shows a 20 cm greyscale plot of a 20' region near the TeV source HESS J1813-178. The TeV centroid is marked with a circle whose radius is equal to the 1' positional uncertainty in the source centroid. The source is reported as extended, with a Gaussian fit yielding $\sigma = 3'$. We have drawn a circle with a diameter of 3' to highlight the circular shell of ra-

Electronic address: djh@astro.columbia.edu

Electronic address: bob@igpp.ucllnl.org

Electronic address: rlw@stsci.edu

¹ The composite SNR G0.9+0.1 (Helfand & Becker 1987) was also detected by HESS during a pointed observation of the Galactic Center (Aharo-

nian et al. 2005b) but it falls below the threshold of the HESS plane survey.

² The VLA is operated by the National Radio Astronomy Observatory which is a facility of the National Science Foundation operated under cooperative agreement by Associated Universities, Inc.

³ The MAGPIS images are all publicly available on the MAGPIS Web site at <http://third.ucllnl.org/gps>.

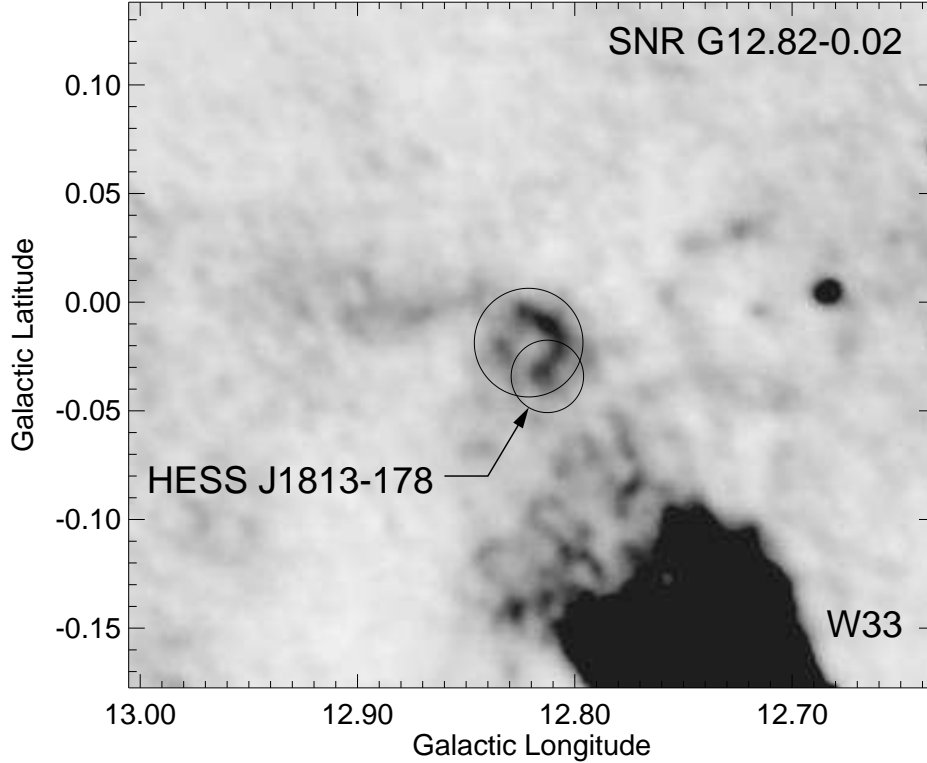


FIG. 1.— VLA 20 cm image of the TeV source HESS J1813-178. The $1'$ radius TeV error circle is shown, and the supernova remnant G12.82-0.02 is marked by a $3'$ diameter circle. The bright nearby H II region W33 can be seen at the lower right.

dio emission centered at RA(J2000) = 18 13 35.5, Dec(J2000) = -17 49 40 (G12.82-0.02); the center of this shell is within $1'$ of the TeV centroid.

This three-array-plus-single-dish image is a superset of the data analyzed by Brogan et al. (2005) who recently reported the discovery of this source. Within the uncertainties, our derived flux density value is consistent with theirs: $S_{20} = 650$ mJy. Only ten of the 231 remnants in the most recent SNR catalog (Green 2004) are this faint. We also made a 90 cm map from the archived data of Brogan et al. and independently completed an analysis of the *ASCA* image containing this source; again all our results are consistent with theirs within the uncertainties, so we need not reiterate the results here. We note, however, that we see no evidence for the X-ray “soft excess” claimed by Ubertini et al. (2005) which is somewhat implausible given the high column density to the source.

3. DISCUSSION

3.1. The environment of G12.82-0.02

G12.82-0.02 lies $\sim 8'$ above (in Galactic latitude) the core of the bright star-forming region W33. First studied in detail by Haschick & Ho (1983), the massive star cluster powering this complex of H II regions has a total Lyman continuum ionizing flux of $> 10^{50}$ photons s^{-1} . From NH_3 observations, the authors infer gas densities of $n(H_2) > 10^4$ cm^{-3} and a total gas mass of $\sim 10^5 M_{\odot}$. Several masers have been detected towards W33; the dominant velocity is ~ 36 km s^{-1} leading to a (near) kinematic distance of ~ 4 kpc. Brogan et al. (2005) cite further evidence that G12.82-0.02 is associated with this star formation complex. At this dis-

tance, the source’s intrinsic (unobscured) X-ray luminosity $L_X(0.1-10 keV) = 5 \times 10^{34}$ erg s^{-1} , and the gamma-ray luminosity $L_{\gamma}(> 200 GeV) = 1 \times 10^{34}$ erg s^{-1} . The radio luminosity is $L_r(10^7 \text{ to } 10^{11} \text{ Hz}) = 3.6 \times 10^{32}$ erg s^{-1} (Brogan et al. 2005).

3.2. Gamma-ray emission mechanisms

Several possible emission mechanisms can lead to TeV gamma-ray emission: a) Inverse Compton scattering by off highly relativistic electrons of ambient starlight, the Cosmic Microwave Background, and/or thermal dust photons, b) non-thermal bremsstrahlung of these same electrons, and c) pion production in p-p collisions followed by Π^0 decay. The high-energy primaries are thought to arise from diffusive shock acceleration in the outward moving blast wave from the supernova event. Lower energy electrons produced in the same process power the observed radio emission. Thus, it is not implausible that there should be some relation between the radio and TeV fluxes of remnants.

3.3. Inverse Compton Emission

In discussing the TeV emission from the composite SNR G0.9+0.1, Aharonian et al. (2005b) produce a model in which the X-rays arise as synchrotron emission by relativistic electrons in the pulsar wind nebula, and the gamma rays arise from inverse Compton scattering of dust IR photons, the cosmic microwave background, and ambient starlight off these same electrons. The starlight dominates at the low energy end of the gamma-ray band, while the CMB photons dominate at the high energy end (the dust emission provides less than a 10% contribution at all energies). The assumed starlight energy density in the Galactic Center region is $5.7 \text{ eV } cm^{-3}$ and

the gamma-ray flux of the source is $f_\gamma(> 200\text{GeV}) = 2.3 \times 10^{-12} \text{ erg cm}^{-2} \text{ s}^{-1}$ at 8.5 kpc; if moved to the 4 kpc distance of G12.82–0.02, the flux would be $10.4 \times 10^{-12} \text{ erg cm}^{-2} \text{ s}^{-1}$.

If we assume the starlight energy density in the vicinity of G12.82–0.02 is dominated by the UV flux from W33, we have

$$\epsilon(\text{starlight}) = LE_\nu / 4\pi d^2 c, \quad (1)$$

and for $L = 10^{50} \text{ ph/s}$, $E_\nu = 15 \text{ eV}$, and $d = 12 \text{ pc}$ (the core of the H II region is $12'$ away), $\epsilon(\text{starlight}) \sim 3 \text{ eV cm}^{-3}$ or roughly half the value for G0.9+0.1. Ambient Galactic starlight might increase this value by $\sim 25\%$, while extensive local obscuration by dust will reduce it by an unknown amount. The gamma-ray flux of $5 \times 10^{-12} \text{ erg cm}^{-2} \text{ s}^{-1}$ is also roughly half the value for G0.9+0.1. Thus, within the rather large uncertainties associated with several of these quantities, the synchrotron X-ray/IC gamma-ray model appears to provide a consistent explanation for the high-energy emission from G12.82–0.02 (cf. Figure 3 of Brogan et al. (2005) where the IC model using CMB photons alone ($\sim 1 \text{ eV cm}^{-3}$) falls roughly a factor of three below the observations, consistent with the three-times higher photon density implied by the proximity of W33). Since the CMB photons provide a somewhat larger fractional contribution in the case of this source, one prediction of this explanation is that the gamma-ray spectrum of G12.82–0.02 should be somewhat flatter than the $\Gamma = 2.4$ found for G0.9+0.1. The view of Brogan et al. (2005) that pion production from accelerated hadrons produces the TeV flux is also tenable.

3.4. What makes TeV remnants?

The discovery of the radio counterpart to HESS J1813–178, along with the non-detection of several radio-bright remnants in the HESS Galactic plane survey demonstrate a large spread in the radio-to-TeV flux ratios for remnants. Adopting as a HESS survey threshold the photon fluxes of the faintest sources detected, $S(> 200\text{TeV}) = 9 \times 10^{-12} \text{ ph cm}^{-2} \text{ s}^{-1}$, and a spectral index of $\Gamma = -2.4$ yields a flux threshold of $3.6 \times 10^{-12} \text{ erg cm}^{-2} \text{ s}^{-1}$ at the Galactic plane. We use the sensitivity curve in Figure 2 of Aharonian et al. (2005a) to scale up the limits with increasing Galactic latitude.

In Table 1, we provide data on several remnants including the detected TeV sources and some of the brighter radio remnants which are not seen. We derive radio fluxes at 1 GHz from the Green (2004) catalog, assuming a uniform radio spectral index of $\alpha \sim -0.65$ and integrating from 10^7 to 10^{11} Hz . Changing the assumed value of α over the observed range for shell-type remnants from 0.4 to 0.8 translates to a flux density range of a factor of 2.5. Gamma-ray fluxes ($E > 200 \text{ GeV}$) are taken from the sources cited; upper limits for sources undetected in the HESS plane survey are set at the flux of faintest detected objects. The final column of the table lists the ratio of radio to gamma-ray flux. There is an extraordinary range of nearly a factor of 10^4 in this value.

There is no obvious correlation of the TeV-radio flux ratio with angular or physical remnant size or with radio spectral index; e.g., G6.4–0.1 and G8.7–0.1 are within a factor of two of the same diameter and have similar spectral indices of $\alpha \sim 0.5$ and yet differ in their flux ratios by a factor of 16. What parameters do the TeV-emitting sources have in common?

Of the six detected remnants in the HESS survey area, two (G347.3–0.5 and G12.82–0.02) have X-ray spectra dominated by a power law component assumed to arise in synchrotron emission associated with the SNR shell, while a third

(G0.9+0.1) has a central pulsar wind nebula that also emits synchrotron X-rays; the other three remnants have not been studied at X-ray wavelengths. Of the remnants undetected by HESS listed in Table 1, thermal X-ray emission dominates in G6.4–0.1, G21.8–0.6 was marginally detected by *Einstein*, and has not been observed since, and G348.5+0.1 is undetected in X-rays. However, X-rays have been detected from some two dozen other remnants in the survey area and eighteen are dominated by soft, thermal emission. There is a clear preference for TeV emitters to also show substantial synchrotron X-ray emission implying the presence of electrons with energies significantly in excess of 100 TeV; likewise, strong synchrotron X-ray emission is lacking in many of the undetected remnants.

Another set of SNRs that are known to have synchrotron X-ray spectra are the pulsar wind nebulae (PWNe) and composite objects that contain a PWN. The parameters of PWNe falling in the HESS survey are listed in Table 2 (including the HESS-detected SNR G0.9+0.1, which is repeated from Table 1.) The gamma-ray upper limits in the 0.2–10 TeV band are derived as described above. The X-ray data are taken from the literature and scaled to be unabsorbed fluxes in the 0.5–10 keV band. The radio flux densities are for 20 cm; in composite remnants, the X-ray and radio values are for the PWN only. G12.82–0.02 is included as the last entry in the table for comparison.

If gamma rays were in general produced by hadronic processes, one might naively assume there would be some relationship between the radio flux density of a remnant which ultimately arises from the particle acceleration process, and the gamma-ray flux. However, as noted above, the brightest radio remnants remain undetected while some of the faintest remnants are seen. For example, in Table 2, the radio flux densities and gamma-ray fluxes for G0.9+0.1 and G12.82–0.02 seem unrelated; G0.9+0.1 is seven times brighter in the radio and only half as bright in the TeV range. However, examining the X-ray and gamma-ray fluxes in the context of an inverse Compton model for gamma-ray emission appears somewhat more promising.

The final column of Table 2 lists limits on the flux density νf_ν in starlight at the PWN under the assumption that the IC model presented in Aharonian et al. (2005b) for G0.9+0.1 is correct, and the highly simplified additional assumption that the gamma-ray-to-x-ray flux ratio for these sources is universal except that it scales with the ambient starlight flux; i.e.,

$$f_\gamma / f_x = 0.05 f_{\text{opt}}, \quad (2)$$

where the constant is derived from the parameters of G0.9+0.1. It is apparent that these assumptions are not seriously challenged by the available data. As noted above, the *observed* value of the ambient flux from the H II region W33 is sufficient to explain the gamma-rays from G12.82–0.02 with this relation. Furthermore, all the other PWN have upper limits on their starlight fluxes that are plausible; most are far above the high value of $2 \times 10^{-12} \text{ erg cm}^{-2} \text{ s}^{-1}$ found near the Galactic Center. Only G21.5–0.9 is significantly lower; it is even slightly below the value for G12.82–0.02, but an examination of the region surrounding this remnant shows no bright H II regions lie within $10'$ and, given the source's location nearly one degree off the Galactic plane, this lower starlight flux is expected.

4. CONCLUSIONS

One of the blank-field TeV-emitting gamma-ray sources in the HESS Galactic plane survey is firmly identified with a

TABLE 1
RADIO AND GAMMA-RAY PROPERTIES OF SELECTED REMNANTS

SNR	Size (arcmin)	Distance (kpc)	f_r (10^{-12} erg cm $^{-2}$ s $^{-1}$)	f_γ (10^{-12} erg cm $^{-2}$ s $^{-1}$)	f_γ/f_r
G0.9+0.1	8	8.5	2.5	2.3	0.9
G6.4-0.1 (W28)	48	2	43	< 3.6	< 0.1
G8.7-0.1 (W30)	26	6	11	16	1
G12.82-0.02	3	4	0.2	12	60
G21.8-0.6	20	> 6	9.5	< 3.7	< 0.4
G23.3-0.3 (W41)	38	5	9.6	13	1
G338.3-0.0	8	...	1.0	19	20
G347.3-0.5	60	6	> 0.5	250	< 500
G348.5+0.1	15	10	10	< 3.6	< 0.4

NOTE. — This table includes SNRs in the HESS survey that are detected as TeV sources and/or are radio bright. The fluxes are for 0.2–10 TeV (f_γ) and 10^7 – 10^{11} Hz (f_r).

TABLE 2
X-RAY, GAMMA-RAY, AND RADIO PROPERTIES FOR PULSAR WIND NEBULAE IN THE HESS SURVEY

SNR	Gamma-ray Flux (10^{-12} erg cm $^{-2}$ s $^{-1}$)	X-ray Flux (10^{-12} erg cm $^{-2}$ s $^{-1}$)	Radio Flux Density (Jy)	Flux in Starlight (10^{-12} erg cm $^{-2}$ s $^{-1}$)
G0.9+0.1	2.3	22	4.5	2.1
G11.2-0.3	< 3.7	10	0.36	< 7.4
G16.7-0.3	< 3.7	2	0.12	< 37
G20.0-0.2	< 3.6	1	9.7	< 72
G21.5-0.9	< 4.5	110	6.0	< 0.8
G29.7-0.3	< 3.9	40	0.28	< 2.0
G343.1-2.3	< 9.0	0.005	0.03	< 3×10^4
G12.82-0.02 ^a	5.2	115	0.65	0.9

NOTE. — This table includes SNRs in the HESS survey that are PWN. Gamma-ray fluxes are for the 0.2–10 TeV band. X-ray fluxes are for the 0.5–10 keV band. Radio flux densities are at $\lambda = 20$ cm. The X-ray and radio values for composite remnants include only the PWN. Starlight fluxes are νf_ν at 15 eV determined from Eqn. (2).

^aNot known to be a PWN, but included for comparison.

small-diameter, faint, shell-like radio SNR which has an X-ray spectrum dominated by synchrotron X-rays. The gamma-ray flux can be explained by inverse Compton scattering of the starlight from the nearby H II region W33 off the X-ray emitting electrons. The detections and upper limits for the 90 other supernova remnants in the inner Galaxy demonstrate that there is a large range ($> 10^3$) of radio-to-gamma-ray flux ratios, and an association of detectable TeV emission with X-ray synchrotron emission. Examination of the seven pulsar wind nebulae in the survey region demonstrates consistency with the notion that the range of gamma-ray-to-x-ray flux ratios can be explained by variations in the energy density in ambient starlight. Deeper HESS observations, as well as sensitive X-ray observations of the many remnants whose X-ray emission remains uncharacterized will be necessary before

more informed constraints on the TeV emission mechanism can be constructed.

D.J.H. and R.H.B. acknowledge the support of the National Science Foundation under grants AST 02-6309 and AST 02-655, respectively. D.J.H. was also supported in this work by NASA grant NAG5-13062. R.H.B.'s work was supported in part under the auspices of the US Department of Energy by Lawrence Livermore National Laboratory under contract W-7405-ENG-48. R.L.W. acknowledges the support of the Space Telescope Science Institute, which is operated by the Association of Universities for Research in Astronomy, Inc., under NASA contract NAS5-26555.

REFERENCES

- Aharonian, F., et al. 2004a, A&A, 425, L13
 Aharonian, F. A., et al. 2004b, Nature, 432, 75
 Aharonian, F., et al. 2005a, Science, 307, 1938
 Aharonian, F., et al. 2005b, A&A, 432, L25
 Allen, G. E., et al. 1997, ApJ, 487, L97
 Becker, R. H., Szymkowiak, A. E., Boldt, E. A., Holt, S. S., & Serlemitsos, P. J. 1980, ApJ, 240, L33
 Benbow, W., & HESS Collaboration 2005, AIP Conf. Proc. 745: High Energy Gamma-Ray Astronomy, 745, 611
 Brogan, C. L., Gaensler, B. M., Gelfand, J. D., Lazendic, J. S., Lazio, T. J., Kassim, N. E., & McClure-Griffiths, N. M. 2005, ArXiv Astrophysics e-prints, arXiv:astro-ph/0505145
 Green, D. A. 2004, Bulletin of the Astronomical Society of India, 32, 335
 Haschick, A. D., & Ho, P. T. P. 1983, ApJ, 267, 638
 Helfand, D. J., & Becker, R. H. 1987, ApJ, 314, 203
 Koyama, K., Petre, R., Gotthelf, E. V., Hwang, U., Matsuura, M., Ozaki, M., & Holt, S. S. 1995, Nature, 378, 255
 Muraishi, H., et al. 2000, A&A, 354, L57
 Reich, W., Reich, P., & Fuerst, E. 1990, A&AS, 83, 539

Slane, P., Gaensler, B. M., Dame, T. M., Hughes, J. P., Plucinsky, P. P., &
Green, A. 1999, *ApJ*, 525, 357